Sensors and Materials, Vol. 12, No. 7 (2000) 397–419
MYU Tokyo

S & M 0418

State-of-the-Art High-Volume Infrared Detector in France

Jean Pierre Chatard

SOFRADIR, 43-47 rue Camille Pelletan, 92290 Châtenay-Malabry, France

(Received July 11, 2000; accepted October 4, 2000)

Key words: infrared, IRFPA, HgCdTe, cooled detectors, uncooled detectors, MTF, Sofradir

The performance of an infrared (IR) system is based on a high spatial resolution and on a high thermal resolution. An increase in spatial resolution means an increase in the number of pixels, a decrease in the detector pitch and an increase in the detector pixel modulation transfer function (MTF). Regarding the thermal resolution increase, it will be achieved mainly by an improvement in the maximum quantity of charges, which can be stored in the silicon read-out circuits for 2D staring arrays. At present, only cooled detectors satisfy this need of high-performance detectors, such as 2D arrays with TV format resolution and high sensitivity. In this paper, the trends regarding high-performance are discussed and recent infrared focal plane array (IRFPA) results at Sofradir are presented. Finally, a comparison with uncooled detectors, also processed at Sofradir, is presented to outline the differences between both types of detectors.

1. Introduction

High-performance systems are based on their ability to detect and recognize with a high probability an infrared (IR) target, which can be very far away and/or very small.

This ability must be quantified under a large range of mission operating conditions.

The key parameters of interest to quantify high-performance IR systems are, on the one hand, the resolution of optical systems, which can be expressed by the modulation transfer function (MTF), and on the other hand the thermal sensitivity, which can be expressed by the noise equivalent temperature difference (NETD). The MTF can be combined with the NETD to obtain other figures of merit like the minimum resolvable temperature difference (MRTD), which is the NETD divided by the MTF.

At present, most high-performance IR systems are based on quantum-cooled IR detectors, and especially on HgCdTe detectors, and use TDI linear arrays or 2D arrays with TV format resolution and high thermal sensitivity. In particular, Sofradir offers in series production of state-of-the-art HgCdTe detectors used worldwide in many high-performance IR systems thanks to a unique HgCdTe technology.

Based on these detectors, high-performance is discussed in this paper in terms of spatial resolution and thermal sensitivity. Then, new uncooled detectors like amorphous silicon microbolometers developed by CEA-LETI (LIR) and offered by Sofradir at an industrial level are presented, and their performance is compared to that of the high-performance cooled HgCdTe detectors.

2. Spatial Resolution of Infrared Detectors

For a given optical aperture, the spatial resolution of an imager is linked to the pixel pitch and to the total number of pixels per line and per column. The smaller the pixel pitch, the smaller will be the optical aperture (higher f number, cheaper optics) or the more it will be possible to implement pixels in a given optical aperture. The higher the number of pixels in the field of view is, the sharper the image will be.

Current trends are therefore to push the limits of increasing the array size while decreasing the pixel pitch to maximize the number of pixels per array and also to propose cost-effective FPAs by limiting the increase in FPA dimensions.

2.1 *High number of pixels per array*

Manufacturing detectors with a high number of pixels was for a long time limited by the technology for manufacturing large sensitive surfaces and/or very small pixel sizes and by the capability to read-out the signals with requested multiplexing and frame rates. In the 1980s, the step from first-generation to second-generation infrared detectors opened the way for high-resolution scanned arrays with time delay and integration (TDI) and signal processing within the focal plane. The 288×4 array (see Fig. 1(a)), is proposed for standard TV format resolution using mechanical scanning and odd and even line interlacing (576×768 European format when used as a 288×4, or 480×640 US format when used as a 240×4).

The high-resolution US standard for scanned systems is the monolithic 480×6 (see Fig. 1(b)), chosen for the new US common modules SADA I and SADA II. These systems enable 4/3 and 16/9 TV formats without interlacing and provide HDTV resolution with single interlacing.

The development of TDI scanning arrays in the 8- to 11-μm band (LW) was carried out because LW 2D staring arrays with equivalent performance were not available. Because IR material technology had to mature in terms of surface area and associated quality, and read-out circuit performance had to be increased.

In production, medium-resolution 128×128 HgCdTe IRCMOS arrays are offered with a 50-μm pitch for MWIR (3–4.2 μm, or 3.7–4.8 μm) applications and for LWIR (7.7–10 μm) applications.

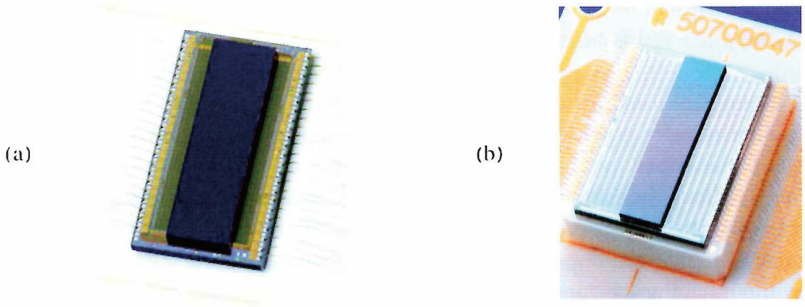

Fig. 1. Sofradir TDI scanning arrays. (a) 288×4 IRCMOS FPA and (b) 480×6 IRCMOS FPA.

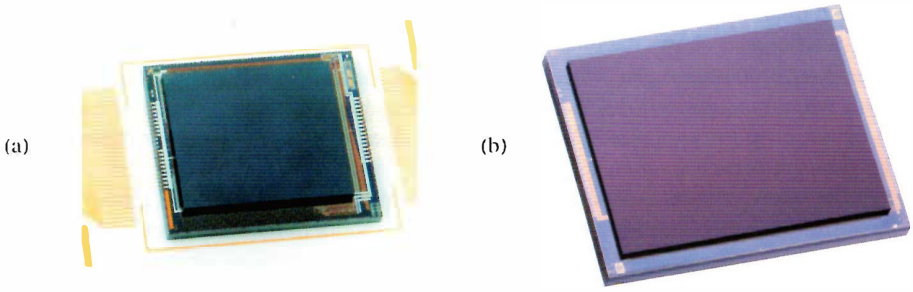

Fig. 2. Sofradir staring arrays. (a) 30-μm pitch (320×256 IRCMOS FPA) and (b) 25-μm pitch (640×480 IRCMOS FPA).

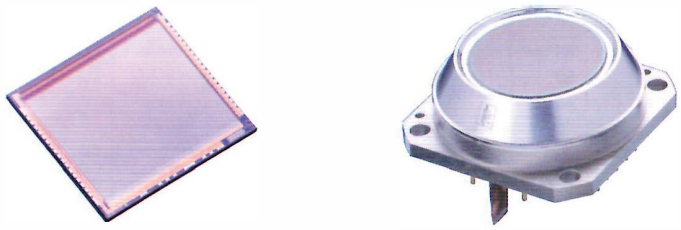

Fig. 21. Sofradir uncooled 320×240 microbolometer detector. (a) 320×240 microbolometer IRFPA and (b) packaging.

The 320×256 format is manufactured with a 30-μm pitch enabling, with the same chip, to choose in addition to the random windowing the standard square 256×256 windowing for seeker-like applications and the US standard TV/4 320×240 format (see Fig. 2(a)). This array is available for SWIR (1–2.5 μm), MWIR (3–4.2 μm, or 3.7–4.8 μm) and LWIR (7.7–9 μm) applications.

The US TV format 640×480 (see Fig. 2(b)) is manufactured in prototype quantities with a 25-μm pitch and is currently offered for MWIR (3.7–4.8 μm) applications.

2.2 *An always decreasing pixel pitch*

To implement more pixels per surface unit, the challenge is to process diodes as small as possible in the array.

The real challenge concerns the staring arrays and not the scanning arrays. Indeed, for the latter, read-out circuit pixels can be shifted to the side of the PV detector (and beside the position of the detective pixels) to implement almost as much signal processing as needed without having the constraint of the staring array pixel size.

The challenge therefore involves the 2D arrays, which require the smallest pitch for all the elements requested by the process or by the system.

Based on the perfect control of the photodiode sensitive area, thanks to the use of ion-implantation processes and the low diffusion length, HgCdTe is the best candidate material for manufacturing very small pitch and therefore for the production of TV format and more. Figure 3 shows the pitch evolution of the 2D arrays manufactured at Sofradir.

The pitch reduction is also linked to the capability of designing and manufacturing 2D arrays CMOS read-out circuits at the expected pitch and with the requested performance in terms of integration and read-out capacitance values, noise and master clock frequency and other parameters.

This is often a challenge to implement a read-out input stage in a small pitch with, for instance, an integrate-while-read mode, a low noise and a maximized (optimized) well-fill.

The evolution of the CMOS foundry technologies for infrared components (with design rules of 1.3 μm, then 0.7 μm, then 0.5 μm, and now 0.35 μm) introduced developments in the designs and the acceptable performance and enables one to propose small pitches with almost constant performance.

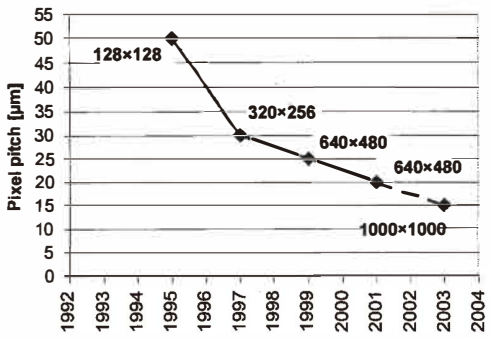

Fig. 3. Decrease of the 2D array standard pixel pitch at the production level.

2.3 *Well-controlled pixel shape*

The ion-implantation process enables precise control of the diode size and shape. Once implantation is performed through a mask, there is a volume diffusion with a diffusion length L_D slightly depending on the cut-off wavelength of the diode. Then, the diode shape follows an exponential decrease according to $\exp(-x/L_D)$ (see Fig. 4). The implantation mask size is determined according to the final required diode size (typically determined as the 50% response points) minus the diffusion length.

Diffusion lengths depend slightly on the cut-off wavelength. However, this technology exhibits small diffusion length values, typically a few microns. Other materials and technologies exhibit much larger diffusion length values.

With such an exponential decrease in the sensitivity, the diode profile is not exactly a step function with a plateau of the size of the 50% response line and with vertical edges.

This has some consequence for the spatial resolution of the components, namely, on the pixel MTF which is slightly degraded compared to a theoretical square diode.

However, thanks to Sofradir technology, the MTF results are very close to the expected step function, as presented in the following.

Sensitive diode areas are measured with a laser spot-scan method. The result is a convolution of the real surface by the small gaussian spot profile. Figure 5 represents the measurement of a pixel response from a 320×256 MWIR array with a 30-μm pitch. As shown in Fig. 5(a), before spot deconvolution, the result is a rounded sensitive area whose 50% response line is inscribed into about a 30×30-μm^2 pitch. After deconvolution (Fig. 5(b)), the real sensitive area is close to square, with sharp decreasing edges, with a 50% response line on the example of a rectangle 28.4×29.2 μm^2 inscribed into a 30×30-μm^2 pitch, which corresponds to a 92.1% filling factor.

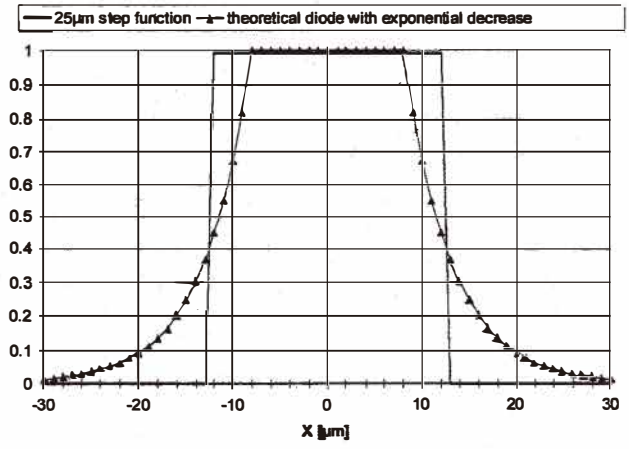

Fig. 4. Theoretical response of a 25-μm ion-implanted diode shape with an exponential decrease $\exp(-x/L_D)$.

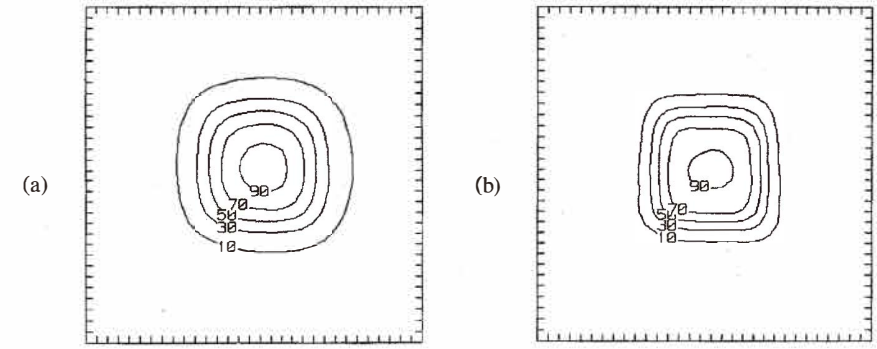

Fig. 5. Measured sensitive area of a 30-μm pitch with ion-implantation process. ($L_x \approx L_y \approx 30$ μm at 50% response $L_x = 28.4$ μm$\times L_y = 29.2$ μm at 50% response => 92% fill factor). (a) before spot scan de-convolution and (b) after spot scan de-convolution.

With such an approach for a high fill factor and close-to-square diodes, it is possible to propose arrays with high-performance spatial resolution since the measured MTF is very close to the theory (which is considered as the step function with a size equal to the array pitch).

2.4 *High-performance MTF*

As shown in Fig. 6, the pixel MTF of LWIR scanning components processed to have a 25-μm pixel size in the in-scan direction is very close to a 25-μm-wide step function.

This is explained by the fact that some diodes are slightly smaller than the nominal requested size and, therefore, the measurement at the theoretical Nyquist spatial frequency corresponds to a spatial frequency lower than the real Nyquist spatial frequency of the diode.

Similarly, the pixel MTF of a MWIR 320×256 staring array is measured very close to the theoretical value, as shown in Fig. 7 (at 16.67 lp/mm = Nyquist frequency, measured MTF≈0.63).

The trends for the pixel pitch of the IR staring arrays is to decrease below 20 μm. The reduced pitch and the well-mastered sharp profile of the pixel, which is very close to the theoretical limit, are key factors to ensure systems with optimized spatial resolution and a very high-performance/price ratio.

3. Thermal Resolution

3.1 *General*

As well as spatial resolution, thermal resolution of infrared detectors is of major interest for system manufacturers, because the thermal sensitivity of a detector is a critical parameter in the definition of the host system (*e.g.,* optical configuration, signal processing, etc.) and its performance (*e.g.,* detection range, etc.).

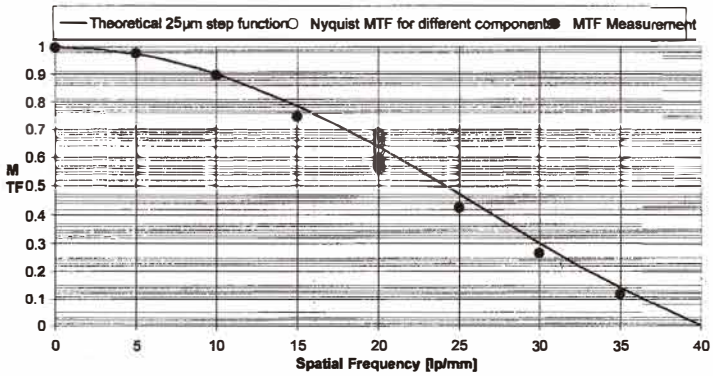

Fig. 6. MTF measurements on LWIR Sofradir components with a 25 μm size diode in-scan specification.

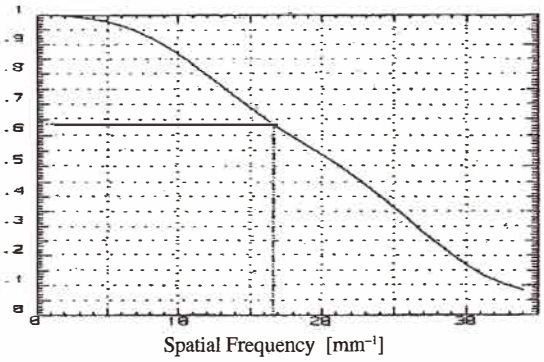

Fig. 7. MTF measurement on a 320×256 MWIR Sofradir component with a 30-μm pixel pitch.

The main function of a detector is to sense infrared radiation coming from a given scene and to deliver an electrical signal proportional to that infrared radiation. Therefore, the performance of a detector is determined by its ability to extract from an infrared background a small target with a temperature close to the background temperature. This ability is generally measured by a figure of merit, NETD (noise equivalent temperature difference) or the detectivity at the detector level.

According to Runciman,[3] the general expression of the NETD of a detector is described by the following equation:

$$NETD = \frac{1}{C\sqrt{N_e}} \times \sqrt{1 + \frac{N_n^2}{N_e}}, \quad (1)$$

with C = luminance contrast, N_e = number of stored electrons and N_n = number of RMS read-out electron noise.

Based on eq. (1), three types of detectors can be defined: detector-noise-limited detectors, photon-noise-limited detectors and charge-storage-limited detectors.

Regarding these different categories, photon-noise-limited detectors have performance close to the theoretical and therefore, for a given application, the thermal performance cannot be increased.

As a matter of fact, for the photon-noise-limited detectors, the performance is driven by the contrast in luminance perceived by the detector; the charge handling capacity is sufficient so that this is not a limitation of the detector. On the other hand, for the charge-storage-limited detectors, the storage capacitance, which is limited in size, limits the detector performance and therefore, for a given application, the thermal performance can be improved.

For detectors with a relatively high read-out noise, the main improvement in the performance relies on the reduction of this noise. This is typically the case for uncooled detectors in which the main limitation is the detector noise (these detectors are not considered in this paragraph).

From a system point of view and for a specific application, the following parameters are given:

- topology of the infrared detector (pitch, etc.)
- spectral waveband (cut-on and cut-off wavelengths)
- sample time and/or maximum integration time
- input flux dynamic range

Therefore, according to the previous discussion, numerous tradeoffs can be made to optimize the detector performance. For example, on the one hand, the MTF can be optimized by reducing the detector active area, as described previously.

On the other hand, a reduction of the active area introduces a reduction in the photodiode signal and therefore a reduction in the number of stored electrons (for a constant integration time). Following eq. (1), the NETD is increased and, therefore, the thermal performance decreased.

Another point that has to be taken into account is the detector spectral bandwidth. Indeed, this spectral bandwidth determines both the luminance contrast in luminance and the photodiode signal (via the generated photonic current). As a consequence, each specific waveband implies specific conditions of use of the infrared detector and, therefore, a specific thermal performance. Depending on its waveband and structure, the detector can be classified either as a photon-noise-limited detector or as a charge-storage-limited detector. For example, generally speaking, a quantum detector is charge-storage-limited in the LWIR waveband and photon-noise-limited in the MWIR waveband (assuming the read-out noise is negligible).

The last point impacting detector performance is the integration time and/or the frame rate. For photon-noise-limited detectors, the higher the integration time, the better the NETD.

Obviously, this parameter does not affect the performance of charge-storage-limited detectors in so far as the storage capacitance of the detector cannot be increased.

In addition to the temporal noise of the detector (NETD), the spatial noise or residual fixed pattern noise (RFPN) of an infrared focal plane array has to be considered by a system user because this is another limiting factor of the detector performance.

Indeed, the RFPN determines the quality of the image homogeneity provided by the infrared detector after nonuniformity correction (NUC). Generally, to take into account the RFPN in a host system, it is compared to the detector temporal noise so that the degradation caused by the RFPN should not be higher than the temporal noise. Thus, the global performance of the system is not degraded by a factor higher than $\sqrt{2}$. Therefore, the better the NETD performance, the better the RFPN of the detector should be, so that the global degradation in the thermal performance of the detector is limited.

In contrast to the temporal noise which cannot be removed by signal processing, the detector RFPN depends on the correction procedure that is used (*e.g.*, 1-point, 2-point or 3-point correction, linear or square correction).

The RFPN can be influenced by many factors such as nonuniformity in detector responsivity, nonlinearity in the read-out circuit, variations in parasitic fluxes with the ambient temperature or the low-frequency noise.

As a consequence, the RFPN evaluation of a detector is given for specific conditions and can be drastically changed according to the conditions of evaluation, the correction procedure and the conditions of use of a detector.

In the following paragraphs, different types of performance of HgCdTe focal plane arrays in terms of temporal noise (NETD) and RFPN are discussed.

3.2 *Linear arrays*

Most applications using mechanical scanning techniques with linear arrays produce infrared images of the observed scene (*e.g.*, FLIRs, seekers, cameras and goggles). Therefore, integration time is generally fixed by system constraints and is very small except in some specific applications (*e.g.*, spectrometry and space applications).

Therefore, linear arrays exhibit outstanding performance for large-flux applications, which is the case in the LWIR waveband where fluxes are much higher than in the MWIR waveband.

As a consequence, due to the short integration time required by applications, linear arrays are photon-noise-limited. For linear arrays, the temporal noise performance is generally increased by implementing TDI stages in the focal plane array.

In the LWIR waveband, a number of 4 to 6 TDI pixels is a good compromise to achieve high-performance without increasing the scanning constraints too much. That is why linear arrays detectors in the LWIR waveband remain competitive compared to staring arrays, which are charge-storage-limited detectors, as described in § 3.3. In the MWIR waveband, the photon flux is much less important than in the LWIR waveband, and therefore, even if the linear detectors are photon-noise-limited, their performance is

not competitive compared to staring arrays (see § 3.3). Typically, 20 to 25 TDI pixels are necessary for linear arrays to recover the same signal-to-noise ratio as staring arrays.

The high quality of these LWIR TDI linear arrays has already been extensively demonstrated and recognized by customers through the quantity of detectors already ordered, delivered and used in operations worldwide. Figure 8 summarizes the detectivity distribution over more than seven hundred 288×4 LW detectors manufactured and delivered representing over 800,000 diodes.

Measurement is expressed in Jones ($cm \cdot Hz^{2/1} \cdot W^{-1}$) for 0.28 sr, 10-$\mu$s integration time and 20°C background temperature.

In Figs. 9 and 10, the main results from a 480×6 focal plane array in terms of detectivity and RFPN measurements are given.

The RFPN correction of the 480×6 detector is performed under the following conditions:

- numerical aperture: f/2.5
- waveband: 7.7 μm–10.3 μm
- correction temperature references: –3°C and 32°C
- integration time: 20 μs
- FPA operating temperature: 80 K

To compare the RFPN value to the previous values of NETD, the RFPN in Fig. 10 is expressed in mK using the following equation.

$$RFPN_{mk}(T) = RFPN_{\mu V}(T) \times \frac{\partial V}{\partial T}, \tag{2}$$

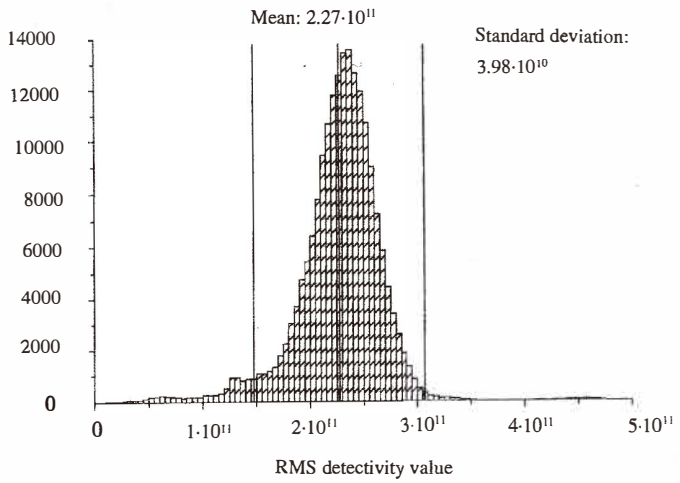

Fig. 8. 288×4 LW Sofradir detector detectivity histogram for more than 700 delivered detectors.

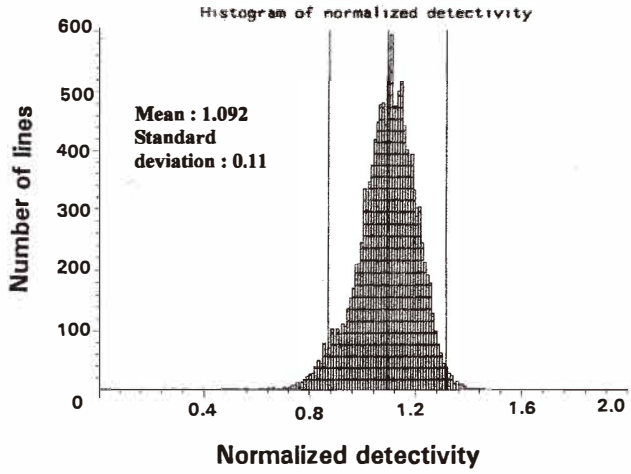

Fig. 9. 480×6 LW Sofradir normalized detectivity histogram for thirty delivered detectors.

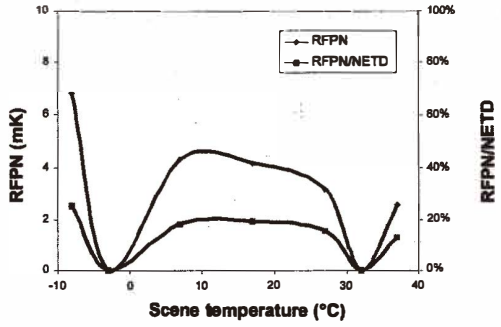

Fig. 10. 480×6 LW Sofradir detector-residual fixed pattern noise (RFPN) and NETD vs scene temperature.

where $\frac{\partial V}{\partial T}$ is the derivative of the average output voltage of the focal plane array vs the scene temperature.

A curve showing the ratio of RFPN and NETD is added in Fig. 10 to compare the RFPN to the NETD vs temperature when a two-point corrections is applied.

Then, in the worst case, this ratio is not higher than 20%, which means that the RFPN is not higher than 20% of the detector average NETD. As a consequence, the degradation in detector performance due to the RFPN is very low.

These different graphs highlight the quality of HgCdTe material required to reach high-performance for both temporal and spatial thermal noises.

Finally, it is worthwhile to note that systems which use scanning mechanisms associated with linear focal plane arrays can carry out frequent updates of correction tables of IRFPA spatial nonuniformity in a frame so that the RFPN of the detector does not degrade as a function of time due to changes in environmental conditions.

3.3 *Staring arrays*

Staring arrays are more and more preferred for infrared systems. However, as discussed previously, depending on photon flux conditions (*e.g.*, field of view and waveband among others) and frame rates, staring arrays may be charge-storage-limited or photon-noise-limited.

Depending on the performance limitations of the staring arrays (meaning the conditions of use, flux, frame rate, and others) and the detector characteristics, the way to optimize the detector performance or the selection of a type of detector may differ.

3.3.1 *LWIR waveband*

In this waveband, HgCdTe staring arrays are generally charge-storage-limited and, therefore, their main limitation is the maximum amount of storable charges, which is linked to the pixel pitch. For a 320×256 focal plane array with a 30-μm pitch, a storable charge of 5.9 pC may currently be achieved.

In Fig. 11, the evolution of the NETD of a 320×256 LW staring array as a function of integration time and cut-off wavelength (for λ_{co} = 7.7 μm) is presented. This graph demonstrates that LWIR HgCdTe staring arrays are generally charge-storage-limited (NETD is constant and its improvement relies on an increase in the storage capacitance) and in consequence, the improvement in thermal performance with respect to LWIR TDI linear arrays is limited (about a factor of two regarding the temporal NETD). This graph

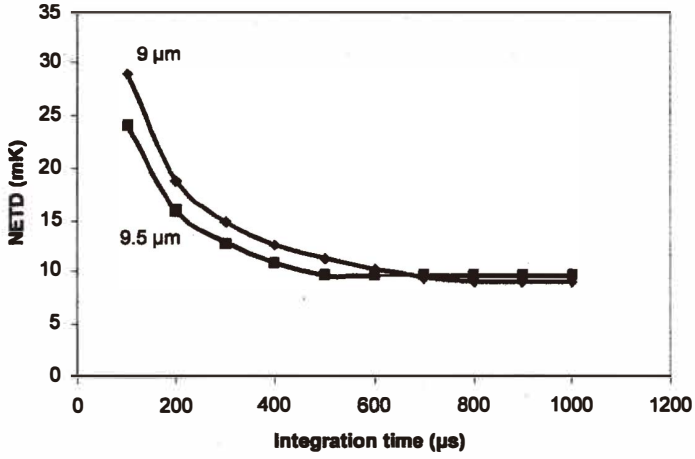

Fig. 11. NETD evolution vs integration time and cut-off wavelength.

also demonstrates that HgCdTe LWIR staring arrays are very competitive for fast frame rate applications (where integration time is reduced), especially in the case of narrow spectral bandwidths.

The dark current of the detector is another limitation to be introduced at the detector level. Indeed, it is also a limitation because this current limits the charge handling capacity and increases the detector noise.

The great advantage of the HgCdTe material is that it allows the cut-off wavelength of the detection circuit to be finely tuned, resulting in a minimization of the dark current vs photonic current. This enables a possible increase in the operating temperature without degradation of the NETD. Otherwise, a reduction of the dark current can be obtained by either decreasing the operating temperature of the focal plane or by decreasing the cut-off wavelength by adjusting the HgCdTe composition. Figure 12 shows a curve describing NETD as a function of the operating temperature of the focal plane and the cut-off wavelength. On this graph are also added curves indicating performance of the same array with an optimized process regarding dark current reduction.[4–6] In Fig. 13, a detectivity histogram of a 320×256 LWIR array with 9.5-μm cut-off wavelength and a 30-μm pitch is shown.

These figures demonstrate that, in the LWIR waveband, the dark current limitation of the performance can be eradicated by either reducing the cut-off wavelength of the array or by using an improved process and, therefore, the thermal performance of the array remains background-limited.

3.3.2 *MWIR waveband*

The MWIR waveband is generally broken down into two sub-bands because of the specific atmospheric transmission conditions.

Thus, HgCdTe focal plane arrays can be used in two major detection waveband categories: between 3.0 μm and 4.2–4.3 μm, and between 3.7 μm and 4.8–5 μm.

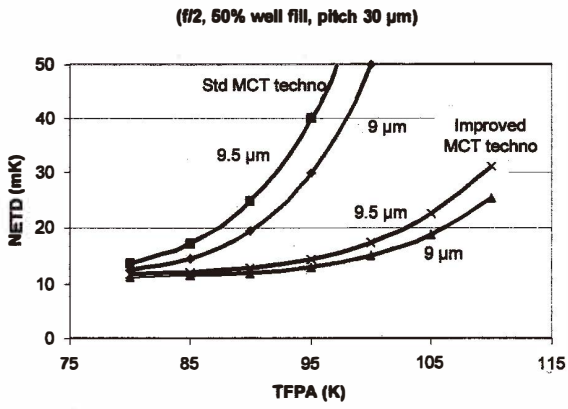

Fig. 12. NETD evolution vs focal plane operating temperature and cut-off wavelength.

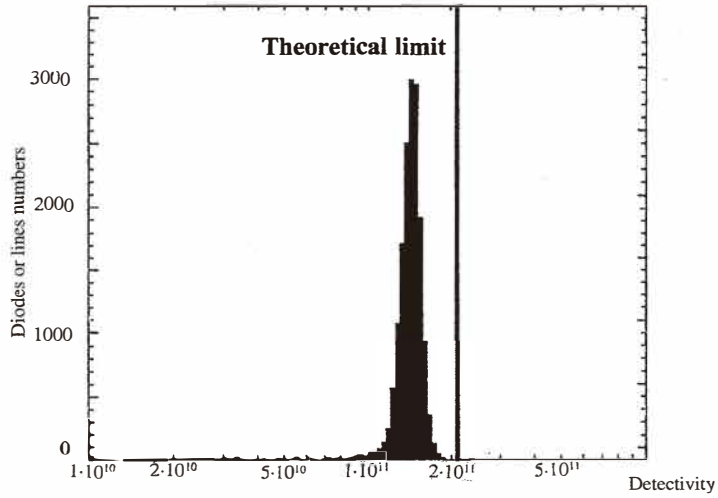

Fig. 13. Detectivity histogram of a 320×256 Sofradir LWIR array.

In these wavebands, the dark current is much less important than in the LWIR waveband[6] and therefore the focal plane temperature can be allowed to rise up to 110 K or 120 K with the same high-performance. Nevertheless, the flux level associated with these wavebands is much lower (for constant numerical aperture) than in the LWIR waveband. Furthermore, the reduction of optical diameter and therefore of optical numerical aperture is a general trend which leads to a reduction in flux.

As a consequence, in the MWIR waveband, staring arrays are photon-limited for most of the applications. This behavior is far more important when microscanning is carried out to increase camera spatial resolution because, of course, the integration time is reduced.

As a result, two main types of flux ranges can be identified in the MWIR waveband: standard fluxes with a medium numerical aperture and relatively large waveband, and low fluxes with a large numerical aperture and/or narrow waveband. To answer these applications, two types of 320×256 focal plane arrays with a 30-μm pitch have been developed:

- A focal plane array with two selectable storage capacitances, a large one (5.9 pC) and a medium one (2 pC), and a low read-out noise,
- A focal plane array with selectable small storage capacitances (0.24 pC), a low read-out noise and an adapted read-out circuit input stage to read very low signal levels.

In the following paragraphs, results from the 320×256 focal plane arrays presented above are given along with evaluations of fixed pattern noise.

3.3.2.1 *3.7 to 4.8 μm bandwidth*

In this waveband, the cut-off wavelength of HgCdTe material is typically tuned above 5 μm so that the cut-off wavelength of the detector is obtained using a cold filter, which in turn, gives IRFPA manufacturing flexibility.

With a medium numerical aperture, the first focal plane array can be offered with a storage capacitance adapted to the charges to store as a function of integration time. A decrease in optical diameter can be done by the system manufacturer and, therefore, the first of the two 320×256 focal plane arrays described above used with the medium storage capacitance is well-adapted to the need.

Figure 14 presents the NETD of a 320×256 MWIR focal plane array (with 30-μm pitch) as a function of the operating temperature for two typical optical apertures (f/2 and f/4). Figure 15 presents a histogram of cumulated NETDs for this type of focal plane array for more than fifty detectors, representing over four million diodes.

These graphs highlight the high-performance and the reproducibility of HgCdTe technology for MWIR staring arrays. In this waveband, TDI linear arrays are not competitive compared with the staring arrays. Indeed, due to the low flux levels, both staring and linear arrays are photon-limited and, therefore, the higher the integration time, the higher the performance. As a consequence, the integration time is longer for staring arrays than for linear arrays (mechanical scanning being unnecessary for staring arrays), NETD performance is better for staring arrays than for linear arrays (even with the TDI effect).

Furthermore, as discussed in the previous paragraphs, the RFPN performance of detectors must also be considered. Figure 16 presents a measurement of the RFPN of a 320×256 focal plane array (30-μm pitch) under the following conditions:

- numerical aperture: f/2
- waveband: 3.4 μm–4.8 μm
- correction temperature references:
  - 20°C and 55°C for two-point nonuniformity correction
  - 20°C, 35°C and 55°C for three-point nonuniformity correction.

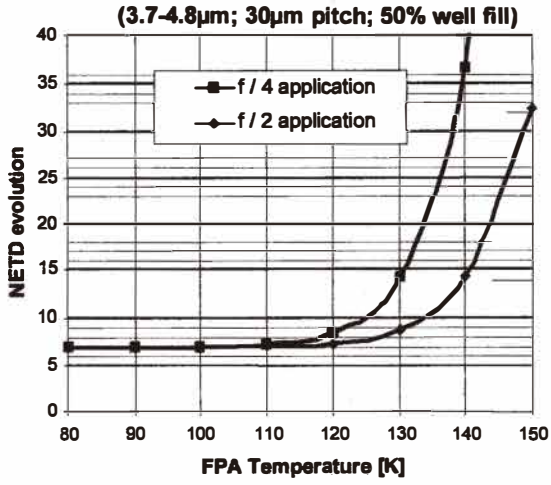

Fig. 14. NETD evolution vs FPA temperature.

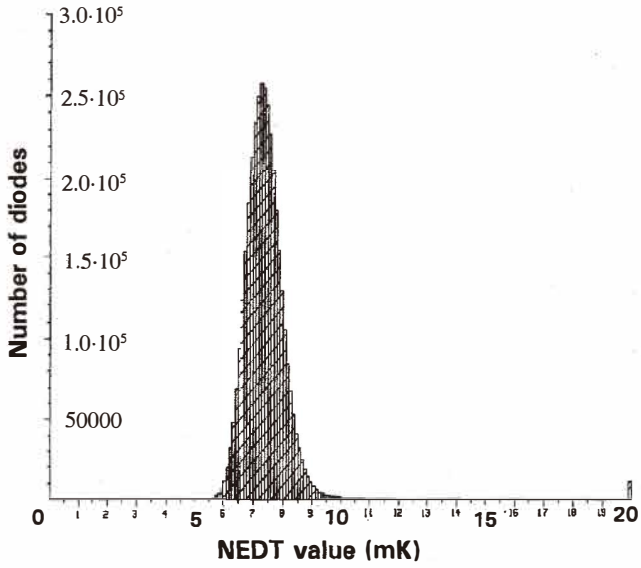

Fig. 15. Cumulated NETD of more than fifty 320×256 Sofradir MWIR detectors.

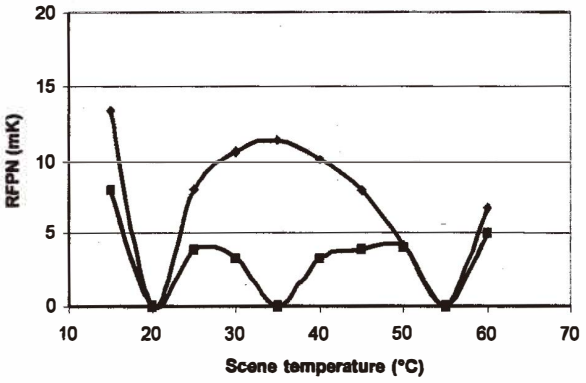

Fig. 16. RFPN of a 320×256 MWIR Sofradir FPA with 2 point NUC (◆) and 3 point NUC (□).

In these graphs, integration time is fixed so that the well fill is 75% for the maximum scene temperature (60°C) and the data acquisitions for the two- or three-point nonuniformity corrections (NUC) are averaged over 16 frames to reduce the effect of temporal noise in the focal plane correction measurement.

To limit the degradation of the global thermal performance of the focal plane array, the RFPN must be lower than or equal to the temporal NETD calculated before. Therefore,

using the previous calculation in Fig. 17, the ratio of the RFPN and the NETD is presented as a function of the scene temperature for the conditions given above.

Figure 17 shows that the RFPN represents less than 100% of the NETD. Therefore, the performance of the staring array is not degraded by spatial nonuniformity. In addition, this figure shows that the three-point correction is better than the two-point correction to reduce RFPN, especially in the case of a large temperature correction range (as in this example, temperature correction range: 45°C).

This last result demonstrates the high quality of the HgCdTe staring array because of a low NETD combined with a RFPN well below the level of the NETD.

3.3.2.2 *3.0 to 4.2-μm bandwidth*

In this waveband, the cut-off wavelength of the HgCdTe material is typically tuned to about 4.3 μm so that the dark current of the detector is lowered to improve the NETD performance. Moreover, in this waveband, staring arrays are always photon-noise-limited because the constraints regarding flux and integration time are more stringent for this waveband than in the 3.7- to 4.8-μm waveband.

Therefore, for applications in this bandwidth, a focal plane with a high gain or with a very small storage capacitance coupled with an adapted read-out circuit structure is needed to read low flux information from the detection circuit.

Figure 18 presents the NETD of a 320×256 focal plane array with a 4.2-μm cut-off wavelength as a function of the operating temperature of the focal plane for two different optical numerical apertures (f/2 or f/4).

In this graph, the effect of the adaptation of the HgCdTe material cut-off wavelength is highlighted and the operating temperature of the focal plane can be increased up to 120 K or 130 K (depending on the optical aperture) without degrading performance.

In addition to these results, the RFPN measurement of the focal plane array is shown in Fig. 19 under the following conditions: numerical aperture: f/4.6, waveband: 3.4–4.2 μm, and two-point correction temperatures (54°C and 60°C).

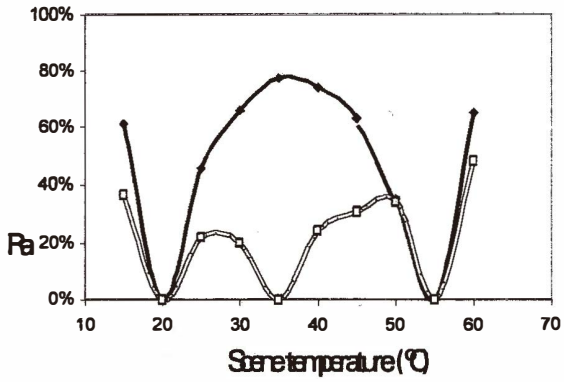

Fig. 17. 320×256 MWIR Sofradir staring array NETD/RFPN ratio with 2 point NUC (◆) and 3 point NUC (□).

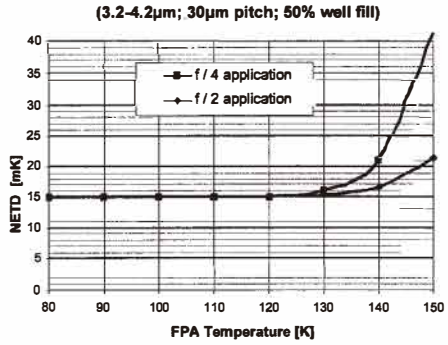

Fig. 18. NETD evolution vs FPA temperature.

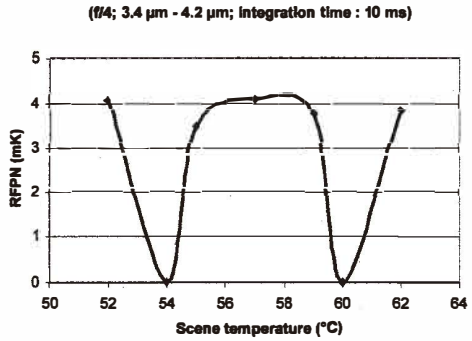

Fig. 19. 320×256 MWIR Sofradir staring array - RFPN measurement.

Integration time is fixed so that the well fill is 50% (for the maximum scene temperature) and the data measurements are averaged over 16 frames to lower the effect of temporal noise.

Therefore, in this waveband, the previous figures demonstrate again the high-performance of the HgCdTe staring arrays and show that the performance is not degraded by RFPN since its maximum value is well below the NETD value.

For this waveband, the challenge is to achieve focal plane arrays with adapted storage capacitances and adapted read-out circuit input stage structures for very low flux levels to limit the degradation of the performance of the detector and to stay in a photon-noise-limited operation.

4. Trends

Sofradir HgCdTe detectors are offered as TDI linear arrays and staring arrays and are representative of the state of the art for high-performance IR detectors.

As a matter of fact, TDI linear arrays and most of the staring arrays are close to the theoretical limit regarding spatial and thermal performance (including RFPN behavior), as described in this paper.

TDI linear arrays are photon-noise-limited and thus achieve at the highest performance level. Their development is now complete, and these arrays have been in series production for many years. The Sofradir 288×4 and 480×6 detector arrays are the basis for many high-performance applications worldwide especially in the LWIR waveband, in which their performance is very competitive with staring arrays.

Regarding staring arrays, their resolution must be improved before achieving a competitive cost with respect to linear arrays.

Thus, the goal of new HgCdTe focal plane array development lies on the one hand in increasing the staring array detector format (TV format and larger) by decreasing the pitch, and on the other hand in increasing the storage capacitance (especially for LWIR arrays) or at least maintaining an equivalent storage capacitance when the pitch is decreased.

The high-performance HgCdTe 320×256/320×240/256×256 IRFPA allows one to choose between the TV/4 US format, the TV/4 European format and the standard square format for seeker-like applications. This Sofradir MWIR detector is in series production today. The same format is also available for SWIR and LWIR applications.

For higher formats, Sofradir has already manufactured and offers high-performance HgCdTe 640×480 MWIR detectors with 25-μm pitch. An example of a 640×480 MWIR focal plane array detectivity performance is given in Fig. 20. To be cost effective, the size of the array must be reduced. For large staring arrays, from TV format to larger ones, the goal of Sofradir is to reduce the pixel pitch down to 20 μm or less.

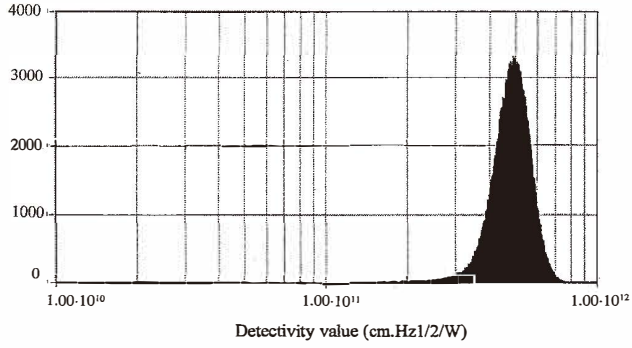

Fig. 20. Detectivity of a 25-μm pitch MWIR 640×480 Sofradir IRFPA.

Regarding silicon read-out circuits, specific developments of new functions are being carried out to improve the performance of focal plane arrays (*e.g.,* linearity for very low flux level, low read-out noise with complex read-out circuit structures) and to simplify the interfaces of the system.

These developments have to cope with the pitch reduction and, therefore, an ever-increasing density of functions is required.

5. Uncooled Detectors

5.1 *General*

The emergence of uncooled detectors has opened new opportunities both for medium performance military and civilian applications. Standard infrared applications are weapons and enhancement of driving vision, low-cost goggles (for military applications), surveillance, nondestructive testing, process control, and hazard warning for vehicles. For many of these applications, the key factor is the cost rather than the performance.

Although the uncooled arrays have a high potential for reducing array costs, the increase in detector performance may also lead to a decrease in system cost. It is therefore interesting to compare uncooled detector performance with cooled HgCdTe high-performance detectors.

5.2 *Sofradir microbolometer detector*

CEA-LETI (LIR) has been involved in the development of amorphous silicon uncooled microbolometers for seven years.[7,8] Following the successful demonstration phase led by the CEA-LETI (LIR), Sofradir has transfered this technology, and a TV/4 product development phase has been conducted under the responsibility of Sofradir (Fig. 21)(p. 399).

The IRFPA of this detector is a 320×240 focal plane array with a 45-μm pitch and a fill factor greater than 80%.

It is sensitive in the long-wave spectral region (8 to 14 μm). The CMOS read-out circuit associated with the amorphous silicon thermometer is from a standard analog CMOS foundry. It enables a pulsed-bias mode of operation of the detector, which enhances both the thermal response of the pixel and the IRFPA immunity to the focal plane temperature variations.

Up to now, as for any thermal detector, the use of vacuum packaging and of a thermal stabilizer remains necessary to achieve good performance by reducing thermal losses and the parasitic effects of the focal plane temperature variations.

The packaging that has been developed (Fig. 21(b))(p. 399) is based on the miniaturization of the assembly linked to the small size of the thermoelectric stabilizer. It is compatible with f/1 optics.

A good vacuum is ensured in the packaging thanks to the use of proven technologies already developed for uncooled detectors. This parameter is of high interest because it enables us to make high-reproducibility, cost-effective products with a low lifecycle cost. One can highlight the main advantages of the amorphous silicon material. Unlike other uncooled microbolometer technologies, it is 100% silicon-process compatible, and it can be processed at high temperatures (> 110°C) during the manufacturing and packaging stages.

This important advantage enables better vacuum conditioning for a longer lifetime without performance degradation, as well as a low-cost process.

Electrooptical characterization of the detectors was performed on the 320×240 IRFPA integrated in the packaging described above with a f/1 optics, 60-Hz-frame rate and 295-K background temperature. The results are presented in Fig. 22(a) and Fig. 22(b).

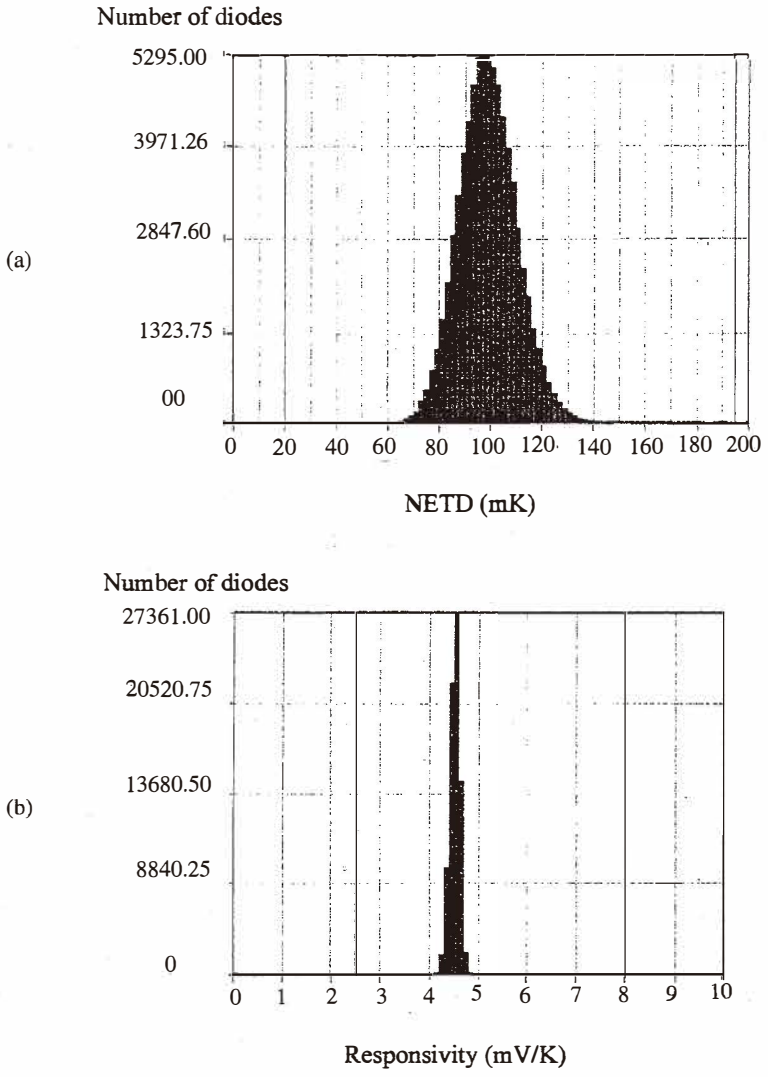

Fig. 22. 320×240 uncooled Sofradir microbolometer performance (f/1, 60 Hz, 295 K background temperature). (a) NETD distribution and (b) responsivity distribution.

The 320×240 uncooled IRFPA demonstrates a responsivity of about 4.5 mV/K with a 3% nonuniformity (standard deviation/mean).

The resulting average NETD is about 100 mK. The operability of these IRFPAs is very good (> 99%), showing the high quality of the technology. It is also interesting to note the good performance of a 100-mK NETD with a 45-μm pitch, which corresponds to 75 mK with a 50-μm pitch.

To lower the NETD figure toward 70 mK with a pitch of 45 μm, several technological improvement studies have already been carried out and these improvements in performance will be implemented in the Sofradir uncooled IRFPA production line.

In addition many tradeoffs can be made to adapt the thermal time constant of the detector to the system requirements and therefore to improve the NETD figure. The goal is to achieve NETD values lower than 30 mK with 50-μm pitch.

From the set of parameters which guided the choices made at CEA-LETI (LIR) and Sofradir, priorities lie in simplifying construction of the microbolometer and its thermal insulation to ensure a quick, easy and low-cost product for industrialization. This was a choice especially adapted for low-cost civilian applications (*e.g.,* goggles, surveillance, process control and driving vision enhancement). The choice of the 45-μm pitch is for the optimization of cost at the level of the IRFPA as well as at the level of the system.

5.3 *Comparison to quantum detectors*

The comparison of uncooled detectors with high-performance quantum detectors deals with spatial resolution and thermal resolution.

The current format of uncooled detectors (320×240) is less than the formats of higher quantum detectors (640×480 to 1000×1000). The current pixel pitch is 50 to 45 μm. Even if a reduction in pitch down to 30 μm is anticipated, these values are still a long way from those of cooled detectors (15 to 20 μm for HgCdTe arrays).

Furthermore, due to poor crosstalk performance, the MTF performance is not as close to theoretical values; the pitch reduction degrades the MTF even more. Therefore, the spatial resolution of uncooled detectors is a long way from that of the HgCdTe cooled detectors.

Regarding NETD performance, 320×240 microbolometers in production give NETD values between 50 mK and 100 mK for 50-μm pitch, f/1 optics and a wide wavelength band (typically 8 to 14 or sometimes even 16 μm). With the same format and conditions the NETD of HgCdTe arrays is a few mK, and therefore the ratio of NETD performance between uncooled detectors and HgCdTe detectors is between 25 and 50 in favor of the HgCdTe.

Considering further improvements in microbolometer technology, the expected performance would be between 10 mK and 30 mK, and thus the ratio of NETD performance with cooled HgCdTe detectors could be in the range from 5 to 15.

If an increase in optical f-number is considered, as microbolometers are detector-noise -limited, the degradation in performance in terms of NETD is directly linked to the reduction of the incoming flux. As an example with f/2 optics, the ratio of the NETD of uncooled microbolometers and cooled HgCdTe NETD would change from 5 to 15 to 10 to 50. Regarding a reduction in pitch, the conclusion is the same.

Finally, one considers that for large format detectors (which supposes a pitch reduction), the NETD ratio between HgCdTe detectors and microbolometers would range between 10 and 50.

Even if the CEA-LETI (LIR)/Sofradir microbolometer technology has a greater potential for pixel pitch reduction than competitive technologies (because of a high fill factor > 80%), the pitch reduction will degrade the MTF as well as the NETD and the final performance will still be far from that of cooled detectors.

Due to the growth of low cost applications, work on uncooled infrared detectors is currently showing rapid changes as a result of developments in silicon technology, which pave the way for the production of low-cost, medium-performance uncooled arrays.

However, based on the combined reductions in spatial and thermal performance, uncooled detectors will not be competitors for high-performance HgCdTe detectors in the next ten years.

6. Conclusions

High-performance IR detectors like HgCdTe detectors are needed to respond to the requirements of high-performance systems in terms of optical and thermal resolution. For most cases, they are very close to the theoretical performance limits. In addition, they are based on mature technologies and may be produced to date in large quantities at Sofradir with a very high-performance-to-cost ratio. The increase in format coupled with a decrease in pitch while keeping constant thermal performance are the trends that will be followed over the next few years to continue to improve the resolution of optical systems. In parallel, technologies involving uncooled IR detectors are progressing very quickly but are still well below those for the cooled detectors in terms of high-performance. However, they will answer the needs of medium-performance systems by reducing system costs and opening very large IR markets, in particular for commercial applications.

References

1 P. Tribolet, J. P. Chatard, P. Costa and A. Manissadjian: J. of Crystal Growth **184–185** (1998) 1262–1271.
2 G. L. Destéphanis: J. of Crystal Growth **86** (1998) 700–722.
3 H. Runciman: Pilkington Optronics, SPIE Proc. **2470** (1995).
4 G. L. Destéfanis: SPIE Proc. **3061** (1997).
5 G. L. Destéfanis and J. P. Chamonal: J. of Electronic Materials **22** (1993).
6 P. Costa and P. Tribolet: SPIE Proc. **3436** (1998) 20.
7 J. L. Tissot, F. Rothan, *et al.*: SPIE Proc. **3379** (1998).
8 C. Vedel, J. L. Martin, *et al.*: SPIE Proc. **3698** (1999).